

# Functionalization of single-walled carbon nanotubes with Prussian blue

Yuanjian Zhang<sup>a,b</sup>, Yi Wen<sup>a</sup>, Yang Liu<sup>a</sup>, Di Li<sup>a</sup>, Jinghong Li<sup>a,b,\*</sup>

<sup>a</sup> State Key Laboratory of Electroanalytical Chemistry, Changchun Institute of Applied Chemistry, Chinese Academy of Sciences, Changchun 130022, PR China

<sup>b</sup> Department of Chemistry, Tsinghua University, Beijing 100084, PR China

Received 26 August 2004; received in revised form 13 September 2004; accepted 14 September 2004

## Abstract

Chemical functionalization of single-walled carbon nanotubes (SWNTs) has constructed plenty of new structures with ample new properties into them. But the modification was often confined to organic molecules, either by covalence or non-covalence. In this report, SWNTs were successfully functionalized with one kind of electroactive inorganic compounds: Prussian blue (PB). And the molecular interactions between them were firstly investigated. Interestingly,  $\pi$ - $\pi$  stacking interaction coupled with ionic interaction was found between SWNTs and PB. The electrochemical properties of SWNTs–PB were also investigated. It would pave a new pathway to manipulate molecular entities of SWNTs by cooperation with functional inorganic electroactive compounds.

© 2004 Elsevier B.V. All rights reserved.

**Keywords:** Carbon nanotubes; Prussian blue; Interaction; Electrochemical properties

## 1. Introduction

Single-walled carbon nanotubes (SWNTs) are one kind of truly molecular entities and their unique properties such as high mechanical strength and chemical stabilities, as well as the relationship between the geometric and the electronic properties have been stimulated to study intensively [1,2]. The manipulations include the solubilization and purification [3,4], derivatization of the tube ends and side [5–9], sorting [10], and assembly [11], etc. Many efforts have been focused on the functionalization of carbon nanotubes with various molecules by using covalent [5,6] and non-covalent approaches [7–9], which have fabricated plenty of new structures with unique functions and applications. But to the best of our knowledge, the functionalization was often con-

finned to organic molecules [5–10]. The inorganic molecules can also interact and cooperate with carbon nanotubes. But this kind of modification, especially with inorganic electrochemical active compounds, was relatively scarce in the literatures [12–15].

Here we introduce one promising electrochemical active inorganic compound, Prussian blue (PB) into SWNTs. PB is a kind of polynuclear and mixed-valent iron cyanide complex with repeating unit of  $\text{Fe}^{\text{III}}[\text{Fe}^{\text{II}}(\text{CN})_6] (\text{Fe}^{\text{III}}\text{HCF}^{\text{II}})$  [16,17]. And the cubic PB structure is not limited to the iron ion and compositions can be varied to include combinations of several transition metal ions in different oxidation states such as Co and Ni [18,19]. Due to the unique properties, synthetic versatility and the ability of the bridging cyanide ligands to efficiently mediate its properties, PB and its analogues have been employed intensively in many fields, such as in the electrochemical [20–23], electrochromic [17,24,25], magnetic [26] and potential analytic applications [27].

\* Corresponding author. Tel./fax: +86 431 5262243.  
E-mail address: [jhli@mail.tsinghua.edu.cn](mailto:jhli@mail.tsinghua.edu.cn) (J. Li).

In this report, PB was attempted to directly functionalize SWNTs and the molecular interactions between them, as well as the electrochemical properties were investigated. Taking the advantage of the unique properties of both SWNTs [28] and PB, it would greatly broaden the applications of SWNTs and PB.

## 2. Experimental

### 2.1. Synthesis

SWNTs were obtained from MER Corporation and purified by suspending the as-received SWNTs with the aid of ultrasonic agitation in a 3:1 v/v mixture of concentrated sulfuric and nitric acid for 1 h. PB was prepared by mixing 100 ml of 0.004 mol/L  $\text{Fe}(\text{NO}_3)_3$  (pH = 1) and 100 ml of 0.004 mol/L  $\text{K}_4[\text{Fe}(\text{CN})_6]$  aqueous solution. After brief stirring, the dark blue precipitate was collected and washed. Then the PB powder was added to SWNTs aqueous solution (typically 100 mg of PB in 10 ml of 0.1 mg/ml SWNTs solution) with vigorous stir for 10 h. After centrifuging, thoroughly washing and drying in vacuum at 50 °C, SWNTs–PB compound was obtained.

SWNTs–PB modified glassy carbon (GC) electrode was prepared by casting 10  $\mu\text{l}$  of 0.1 mg/ml SWNTs–PB suspension on the surface of GC electrode, and was dried in vacuum at 50 °C for 12 h.

### 2.2. Instruments

UV–vis spectra were measured by using UV-360 Spectrometer (made in Japan, Shimadzu).

Transmission electron microscopy (TEM) was performed on JEOL-JEM-2010 (JEOL, Japan) electron microscopy operating at 200 kV. Sample was prepared by casting one drop of the SWNTs–PB suspension onto a standard carbon-coated (200–300 Å) formvar film on copper grid (230 mesh).

Inductively coupled plasma atomic emission (ICP) was measured on POEMS ICP (TJA).

Fourier transform infrared spectroscopy (FTIR) was conducted at FTS135 infrared spectroscopy (BIO-RAD, USA). Transmission spectra of samples was obtained by forming thin transparent KBr pellet containing the interesting materials.

X-ray photoelectron spectroscopy (XPS) was conducted using a VG ESCALAB MK II spectrometer (VG Scientific, UK) employing a monochromatic Mg  $\text{K}\alpha$  X-ray source ( $\nu = 1253.6$  eV). Peak positions were internally referenced to the C1s peak at 284.6 eV.

Resonance raman spectra were measured on Raman Infinity Spectrophotometer (made in France) at a reso-

lution of 4  $\text{cm}^{-1}$ . The 488 nm line with a power of 50 mW from an argon ion laser was used as the excitation source.

Electrochemical measurements were carried out in a conventional three-electrode electrochemical cell. The working electrode was a SWNTs–PB modified GC electrode, the auxiliary electrode was a platinum wire, and the reference electrode was a Ag/AgCl (saturated KCl) electrode. Cyclic voltammetry measurements (CV) were performed with CHI 832 Electrochemical Instrument (CHI Inc., USA).

## 3. Results and discussion

Fig. 1(a) shows the UV–vis spectra of SWNTs, PB, and SWNTs–PB. Both the spectra of PB and SWNTs–PB were dominated by the intense charge-transfer absorption band of the mixed valence  $\text{Fe}^{\text{III}}\text{HC-F}^{\text{II}}$  sequence with a maximum at ca. 700 nm [29]. The fact that SWNTs–PB kept the similar absorption property indicated the successful modification of SWNTs with PB. It was also confirmed by TEM (Fig. 1(b)). The small PB nano-particles (diameter ca. 4 nm) were absorbed around the SWNTs bundles (diameter ca. 20 nm) uniformly. And Fe wt% was ca. 5.54% from ICP analysis.

It was reported that the intrinsic interaction between modifier and SWNTs was either covalence or non-covalence ( $\pi$ – $\pi$  or wrapping). Then what is the intrinsic interaction here between PB and SWNTs? In the microstructure of PB, the ferric ions are coordinated to the nitrogen atoms, and the ferrous ions strongly to the carbon atoms, of the bridging cyanide ligands. It was noticed that both carbon atoms in the sidewall of SWNTs and the CN of PB are conjugated, and then they could act as electron donor and acceptor, respectively. Therefore,  $\pi$ – $\pi$  stacking interaction [7–9] should occur between the sidewall of SWNTs and CN of PB. Besides, cations in the PB (iron ions) might also be ready to interact with anions in the SWNTs (carboxyl moieties [11]) through ionic interaction [4]. In order to confirm these suppositions, the interactions between SWNTs and PB were further investigated by FTIR, XPS, and Raman.

Fig. 2 shows the FTIR of the purified SWNTs (curve 1), SWNTs–PB (curve 2) and bulk PB (curve 3). After purification process, the defects in the sidewall and the open ends of the SWNTs were modified with some carboxyl moieties [11] (Fig. 2, curve 1). And the peak at ca 1400  $\text{cm}^{-1}$  in the spectrum of bulk PB (Fig. 2, curve 2) was due to the  $\text{NO}_3^-$  from the starting material and it disappeared in the spectrum of SWNTs–PB due to additional washing with water. The peaks of the two mixed  $\text{T}_{1u}$  metal–ligand stretching and metal–carbon–nitrogen bending modes in the spectrum of PB (ca.

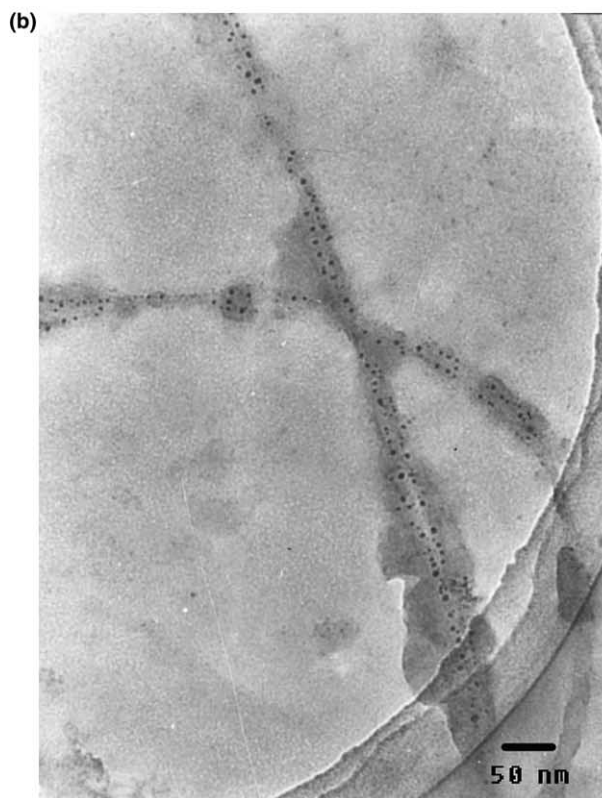
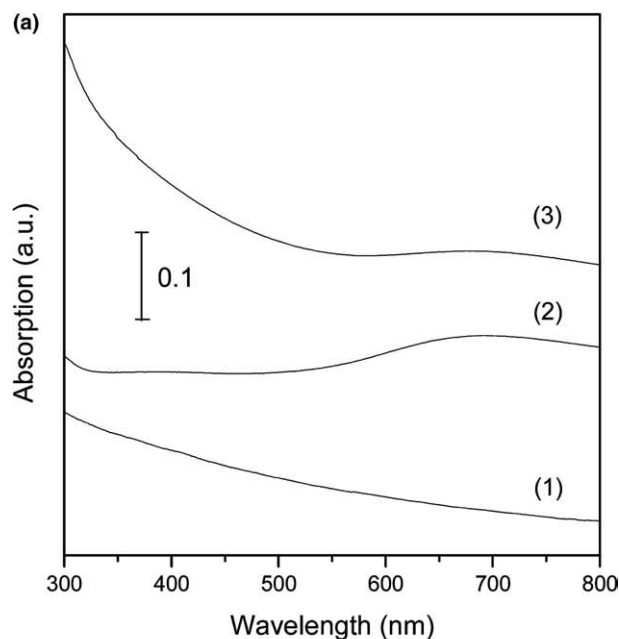


Fig. 1. (a) UV-vis spectra of SWNTs (curve 1), PB (curve 2), and SWNTs-PB (curve 3). (b) TEM image of SWNTs-PB.

602 and 498  $\text{cm}^{-1}$ , respectively) [16,17] changed little in the spectrum of SWNTs-PB (ca. 600 and 500  $\text{cm}^{-1}$ , respectively), which indicated that the environment of both ferric and ferrous ions changed little. However,  $T_{1u}$  CN stretching mode of PB, was affected significantly by SWNTs, which changed from ca. 2085  $\text{cm}^{-1}$  in the

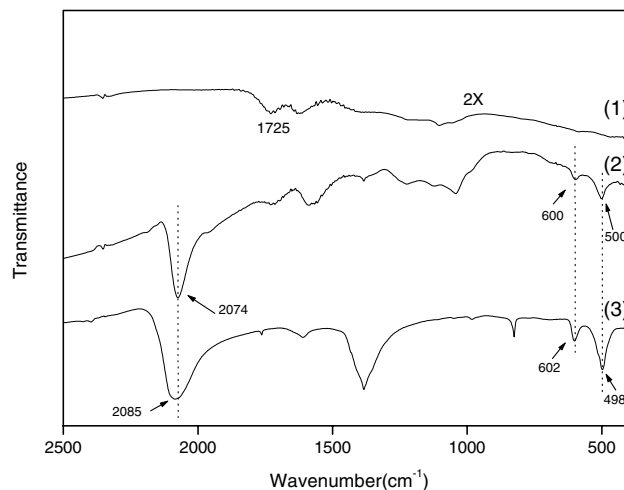


Fig. 2. FTIR of SWNTs (curve 1), SWNTs-PB (curve 2) and PB (curve 3).

spectrum of PB [16–19] to ca. 2074  $\text{cm}^{-1}$  in that of SWNTs-PB.

The CN stretching frequency is quite sensitive to the environments of the bonding, and the frequencies for  $\text{Fe}^{\text{III}}\text{HCF}^{\text{II}}$ ,  $\text{Fe}^{\text{II}}\text{HCF}^{\text{III}}$ , and  $\text{Fe}^{\text{III}}\text{HCF}^{\text{III}}$  were reported as 2070, 2080, and 2111  $\text{cm}^{-1}$ , respectively [18]. It was noted that, the iron ion, which was coordinated with carbon atoms affected the electron density of CN more effectively, and the frequency increased with the decrease of the electron density of CN. The obvious shift of CN stretching frequency here might be due to the acceptance of electron from SWNTs to CN of PB, which decreased the electron density of CN. Therefore, it provided the evidence of  $\pi$ - $\pi$  stacking interaction between SWNTs and PB.

Besides, the XPS measurements were performed to help confirm the presence of  $\pi$ - $\pi$  stacking interactions (Fig. 3). The binding energy of Fe (2p<sub>3/2</sub>), which appeared at ca. 711.1 eV for Fe(III) and 708.1 eV for Fe(II) [11] changed little when PB was modified to SWNTs. However, the binding energy of N (1s) decreased significantly from 397.8 to 397.2 eV and there was some broadening of N (1s) peak after the modification; this was due to CN accepted electrons from the unallocated electrons of SWNTs through  $\pi$ - $\pi$  stacking, which lowered the binding energy of N (1s).

Fig. 4 shows the Raman spectra of SWNTs (curve 1) and SWNTs-PB (curve 2). Both spectra contained characteristic peaks at 1558 and 1584  $\text{cm}^{-1}$  (tangential mode) and at 1343  $\text{cm}^{-1}$  (disorder mode) [3]. As the disorder mode is the diagnostic of disruptions in the hexagonal framework of the SWNTs [3], the fact that the relative intensity of this mode increased provided the direct evidence of the increased disruption of SWNTs. Since the  $\pi$ - $\pi$  stacking interaction would not

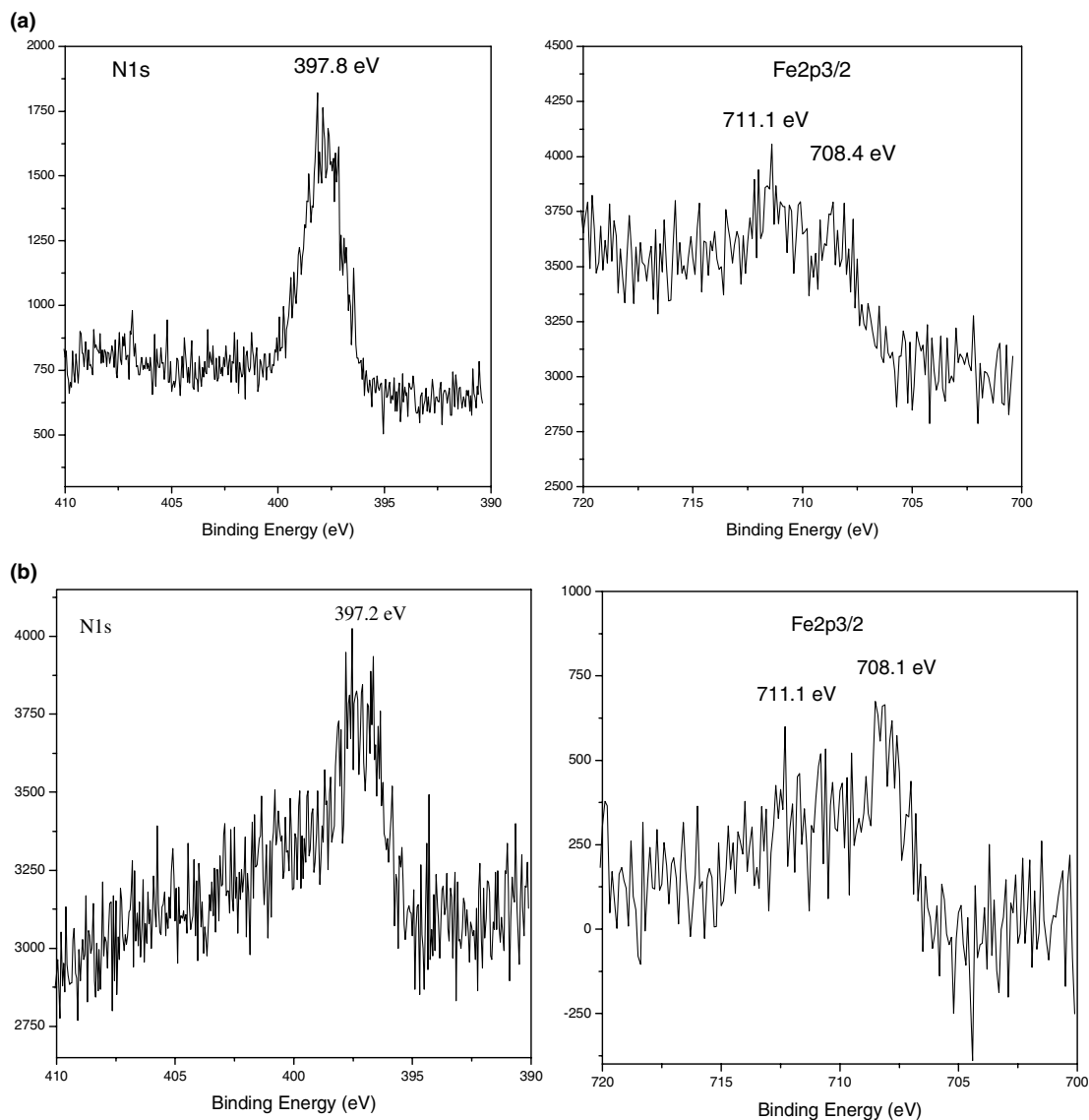


Fig. 3. XPS spectra of (a) PB and (b) SWNTs-PB.

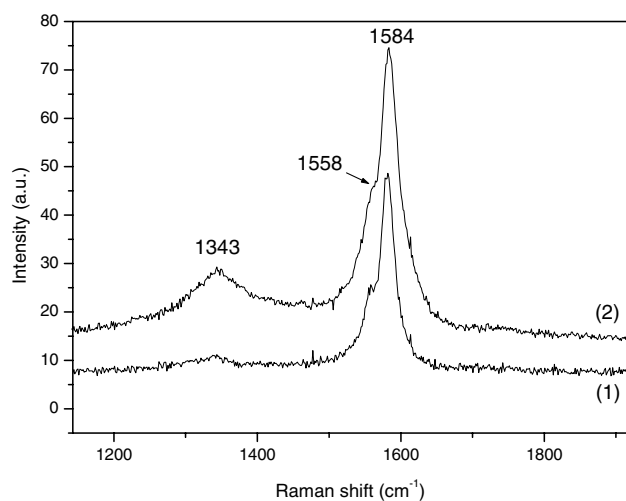


Fig. 4. Raman spectra of SWNTs (curve 1) and SWNTs-PB (curve 2).

bring such changes [3], ionic interaction was also expected.

Due to the unique properties of SWNTs and PB, SWNTs-PB was expected to be widely used, such as the magnetic and electrochemical fields. Fig. 5 shows the CV measurements of SWNTs-PB modified GC electrode in 0.1 M  $\text{K}_2\text{SO}_4$ , which had a couple of well defined redox peaks [20–23]. The former potential,  $E_0$   $[(E_{\text{pa}} + E_{\text{pc}})/2]$  was calculated as ca. 0.20 V (vs. Ag/AgCl) and unchanged with that of PB in the literature [20–23]. And the peak current  $[(I_{\text{a}} + |I_{\text{c}}|)/2]$  increased linearly with the scan rates (Fig. 5 inset), as expected for an electron transfer-controlled redox process. Therefore, SWNTs-PB maintained good electrochemical activity of PB and it could find the applications in the field of electrochemistry.

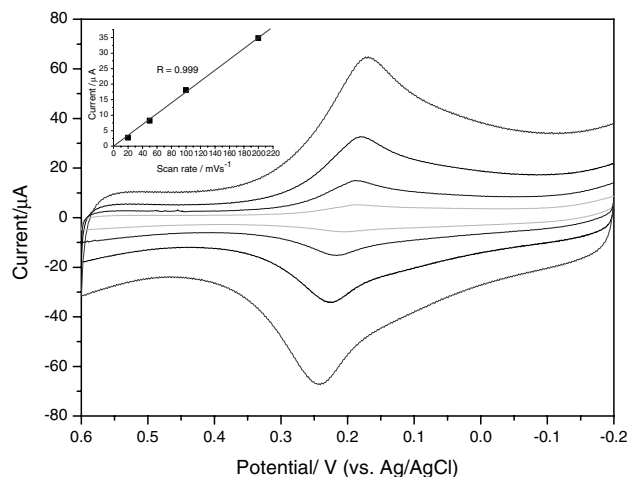


Fig. 5. Cyclic voltammetry of SWNTs–PB modified GC electrode at different scan rates. Inserted is the plot of peak current versus the scan rate. Scan rate: 20, 50, 100, 200 mV/s from inner to outer. Supporting electrolyte: 0.1 M  $K_2SO_4$  solution.

#### 4. Conclusions

In summary, SWNTs were successfully functionalized with PB, and the interactions between PB and functionalized SWNTs were investigated by measurements of UV–vis, TEM, ICP, FTIR, Raman, and XPS. The preliminary results indicated the existence of the  $\pi$ – $\pi$  stacking interaction coupled with the ionic interaction between SWNTs and PB. The electrochemical behavior of SWNTs–PB was also investigated and it was found that PB retained its good redox properties. Taking the advantage of the unique properties of both SWNTs and PB, it would greatly broaden applications of SWNTs and PB. Therefore it would pave a new pathway to manipulate molecular entities of SWNTs by cooperation with functional inorganic electroactive compounds. We are currently investigating the electrochemical, magnetic, and other properties of PB functionalized SWNTs.

#### Acknowledgement

This work was financially supported by the National Natural Science Foundation of China (No. 20125513).

#### References

- [1] P.M. Ajayan, *Chem. Rev.* 99 (1999) 1787.
- [2] S. Iijima, *Nature* 354 (1991) 56.
- [3] C.A. Dyke, J.M. Tour, *Chem. Eur. J.* 10 (2004) 812.
- [4] J. Chen, A.M. Rao, S. Lyuksyutov, M.E. Itkis, M.A. Hamon, H. Hu, R.W. Cohn, P.C. Eklund, D.T. Colbert, R.E. Smalley, R.C. Haddon, *J. Phys. Chem. B* 105 (2001) 2525.
- [5] A. Bianco, M. Prato, *Adv. Mater.* 15 (2003) 1765.
- [6] R. Czerw, Z. Guo, P.M. Ajayan, Y.-P. Sun, D.L. Carroll, *Nano Lett.* 1 (2001) 423.
- [7] J. Zhang, J.-K. Lee, Y. Wu, R.W. Murray, *Nano Lett.* 3 (2003) 403.
- [8] Y. Lin, B. Zhou, K.A. Fernando, P. Liu, L.F. Allard, Y.-P. Sun, *Macromolecules* 36 (2003) 7199.
- [9] M. Shim, N.W. Shi Kam, R.J. Chen, Y. Li, H. Dai, *Nano Lett.* 2 (2002) 285.
- [10] M. Zheng, A. Jagota, M.S. Strano, A.P. Santos, P. Barone, S.G. Chou, B.A. Diner, M.S. Dresselhaus, R.S. Mclean, G.B. Onoa, G.G. Samsonidze, E.D. Semke, M. Usrey, D.J. Wall, *Science* 302 (2003) 1545.
- [11] P. Diao, Z. Liu, B. Wu, X. Nan, J. Zhang, Z. Wei, *Chem. Phys. Chem.* 10 (2002) 898.
- [12] L. Duclaux, *Carbon* 40 (2002) 1751.
- [13] T. Seeger, T. Kohler, T. Frauenheim, N. Grobert, M. Ruhle, M. Terrones, G. Seifert, *Chem. Commun.* (2002) 34.
- [14] B.C. Satishkumar, A. Govindaraj, M. Nath, C.N.R. Rao, *J. Mater. Chem.* 10 (2000) 2115.
- [15] K. Hernadi, E. Couteau, J.W. Seo, L. Forro, *Langmuir* 19 (2003) 7026.
- [16] R.E. Wilde, S.N. Ghosh, B. Marshall, *J. Inorg. Chem.* 9 (1970) 2512.
- [17] D. Ellis, M. Eckhoff, V.D. Neff, *J. Chem. Phys.* 85 (1981) 1225.
- [18] M. Pyrasch, A. Toutianoush, W. Jin, J. Schnepf, B. Tiede, *Chem. Mater.* 15 (2003) 245.
- [19] O. Sato, T. Iyoda, A. Fujishima, K. Hashimoto, *Science* 272 (1996) 704.
- [20] A.A. Karyakin, *Electroanalysis* 13 (2001) 813.
- [21] D. Zhang, K. Wang, D.C. Sun, X.H. Xia, H.Y. Chen, *Chem. Mater.* 15 (2003) 4163.
- [22] D. Zhang, K. Wang, D.C. Sun, X.H. Xia, H.Y. Chen, *J. Solid. State ElectroChem.* 7 (2003) 561.
- [23] P.J. Kulesza, M.A. Malik, A. Denca, J. Strojek, *Anal. Chem.* 68 (1996) 2442.
- [24] R.J. Mortimer, *J. Electrochem. Soc.* 138 (1991) 633.
- [25] P. Somani, A.B. Mandale, S. Radhakrishnan, *Acta Mater.* 48 (2000) 2859.
- [26] P. Zhou, D. Xue, H. Luo, X. Chen, *Nano Lett.* 2 (2002) 845.
- [27] K. Derwinska, K. Miecznikowski, R. Koncki, P.J. Kulesza, S. Glab, M.A. Malik, *Electroanalysis* 15 (2003) 1843.
- [28] C.E. Banks, R.R. Moore, T.J. Davies, R.G. Compton, *Chem. Commun.* (2004) 1804.
- [29] M. Pyrasch, A. Toutianoush, W. Jin, J. Schnepf, B. Tiede, *Chem. Mater.* 15 (2003) 245.